Jurnal Kejuruteraan 38(3) 2026: 1303-1313
https://doi.org/10.17576/jkukm-2026-38(3)-24

High-Capacity 2-Dimensional Modified-FCC Code for Multiple Access Interference Alleviation in Spectral/Spatial OCDMA Systems

Dayang Khadijah[a], Mohd Rashidi Che Beson[a*], Ku Nurul Fazira Ku Azir[a], Bikash Nakarmi[b] & Abu Jubaer Rupok[a]

[a]*Centre of Excellence for Advanced Computing, Faculty of Intelligent Computing,*

Universiti Malaysia Perlis, Kampus Alam, 02600, Arau, Perlis, Malaysia.

[b]*Key Laboratory of RADAR Imaging and Microwave Photonics College of Electronics and Information Engineering,*

Nanjing University of Aeronautics and Astronautics, 29 Jiangjun St, Jiangning, Nanjing, Jiangsu, China. 211106.

[*]*Corresponding author: rashidibeson@unimap.edu.my*

Received 15 September 2025, Received in revised form 18 January 2026
Accepted 18 February 2026, Available online 30 May 2026

ABSTRACT

This study introduces a new structure of spectral/spatial Modified Flexible Cross-Correlation (2-D Modified-FCC) code aimed at enhancing Optical CDMA system by addressing key issues such as MAI and PIIN. In contrast to traditional one-dimensional coding schemes, the proposed method employs a dual-domain approach leveraging both spectral/spatial dimensions to achieve superior cross-correlation characteristics and greater system scalability. The performance results indicated that, at a transmission rate of 1.1 Gbps, the proposed code supports up to 331 simultaneous users, significantly outperforming existing methods for example the 2-D Modified Double Weight and 2-D Perfect Difference code which accommodate only 121 and 39 number of users, respectively. Furthermore, the 2-D Modified-FCC architecture maintains a bit error rate (BER) of 10^{-9} with low received power, Psr = −20 dBm, enabling reliable data delivery over 100 km fiber links without the need for optical repeaters. BER analyses for varying distances (10 km, 70 km, and 100 km) confirm the schemes robustness, yielding BER values of 1.272×10^{-25}, 1.166×10^{-21}, and 4.583×10^{-9}, respectively. These findings suggest that the 2D Modified-FCC code offers a high-capacity, energy-efficient solution suitable for next-generation broadband optical access systems.

Keywords: 2-D Modified-FCC; BER; PIIN; MAI; OCDMA

INTRODUCTION

In optical CDMA scheme, the simultaneous transmission of signals by multiple users can result in significant interference, signal overlapping, and various noise-related issues. Among the dominant noise sources are shot noise, and thermal noise, all of which contribute to the emergence of PIIN, a key factor that limits overall system performance (Din Keraf et al. 2014). PIIN originates from the interference of incoherent optical signals emitted by different users, causing fluctuations in signal intensity that compromise quality. To ensure the scalability and robustness of OCDMA systems, effective mitigation strategies are essential. One promising solution is the adoption of two-dimensional (2-D) coding techniques, which outperform conventional one-dimensional (1-D) schemes by utilizing both spectral and temporal resources for user separation (Redouane et al. 2022) (Abuhelala et al. 2020). In 1-D systems, every subscriber is typically allocated a time or wavelength-based code. However, as the number of users increases, code reuse and overlap become inevitable, escalating the level of interference and diminishing system efficiency (Yousif Ahmed et al. 2020). This added dimensionality enables better noise suppression and improved signal-to-noise ratios (SNR), thereby allowing more users to access the system concurrently with minimal degradation in performance (Boukricha et al. 2020). By contrast, 2-D OCDMA codes employ combinations of wavelength (λ^1, λ^2, ..., λ_m) and time slots (t_1, t_2, ..., t_n) to form more versatile encoding patterns. This

added dimensionality enables better noise suppression and improved signal-to-noise ratios (SNR), thereby allowing more users to access the system concurrently with minimal degradation in performance (Alayedi et al. 2024). Although several 2-D code families such as those developed by (Din Keraf et al. 2014), (Cherifi et al. 2021) and (Mizozoe et al. 2023), they are frequently hampered by drawbacks such as significant code length and difficulty, which hinder their applicability in high-speed link. While some of these designs offer strong correlation properties(Islam et al. 2022), they may fall short in terms of practicality and scalability. To address these limitations, this paper introduces a novel 2-D Modified Flexible Cross-Correlation (Modified-FCC) code. By leveraging a refined interference mitigation mechanism based on spectral-spatial dimensions, the proposed scheme enhances user capacity, reduces PIIN and MAI effects, and improves the overall reliability of the OCDMA system.

ONE-DIMENSIONAL FCC CODE CONSTRUCTION

Optical CDMA systems utilize sets of binary sequences comprising only '1's and '0's assigned to each of the *K* users in the system. These sequences are typical (Morsy, 2022) ly characterized by three parameters: the total length *N*, the number of active bits (or weight) *W*, and the maximum tolerable cross-correlation value λ_{max}. To ensure effective multiple access, the sequences must maintain favorable correlation properties. Specifically, the autocorrelation function should yield a peak at zero delay ($\tau = 0$), while the cross-correlation between distinct users must remain minimal at all other delay values. This is expressed mathematically as proposed by (Tseng et al. 2021).

$$\lambda_x(\tau) = \sum_{i=1}^{N} x_i x_{i+\tau} = W \quad \text{for } \tau=0 \tag{1}$$

$$\lambda_{xy}(\tau) = \sum_{i=1}^{N} x_i y_{i+\tau} = \leq 1 \quad \text{for } \tau\neq 0 \tag{2}$$

where *x* and *y* represent binary sequences of length *N*, and the summations run over the entire sequence length. In practice, one major challenge is the design of these codes such that (Das et al. 2022) concurrent data transmissions do not interfere destructively. This is addressed by constructing sequence sets that reduce overlap among users' codes. Let the binary sequences be denoted by,

$$\left.\begin{aligned} \{x_n\} &= 1 \text{ or } 0, \text{ where, } n = 0,\ldots N-1 \\ \{y_n\} &= 1 \text{ or } 0, \text{where, } n = 0,\ldots N-1 \end{aligned}\right\} \tag{3}$$

The weight, *W* corresponds to the binary one in the sequence when $\tau = 0$,

$$\lambda_x(0) = W \tag{4}$$

To analyze user separability, vector notation can be adopted (Rashidi et al. 2012), where the sequences *X* and *Y* are represented as row vectors of binary values. The correlation measures then become simple vector dot products,

$$\left.\begin{aligned} \lambda_{X(0)} &= XX^T = W \\ \lambda_{XY(0)} &= XY^T \end{aligned}\right\} \tag{5}$$

These vector-based formulations are useful when designing sets of sequences for systems involving multiple users. The complete set of codes can also be represented in matrix form as introduced in Equation (6), offering a structured representation for code allocation and correlation analysis.

$$A_K^W = \begin{bmatrix} a_{i1j1} & a_{i1j2} & a_{i1j3} & 0 & 0 & \cdots & 0 \\ a_{i2j1} & a_{i2j2} & a_{i2j3} & a_{i2j4} & 0 & \cdots & \vdots \\ 0 & a_{i3j2} & a_{i3j3} & a_{i3j4} & a_{i3j5} & 0 & \vdots \\ \ddots & \ddots & \ddots & \ddots & \ddots & \ddots & \vdots \\ \vdots & \vdots & \ddots & \ddots & \ddots & \ddots & \vdots \\ 0 & 0 & \cdots & \cdots & \cdots & \cdots & a_{iKjN} \end{bmatrix} = \begin{bmatrix} A_1 \\ A_2 \\ A_3 \\ \vdots \\ \vdots \\ A_K \end{bmatrix} \tag{6}$$

2-D MODIFIED-FCC CODE ALGORITHM

The 2-D Modified-FCC code is developed by extending the structure of a traditional one-dimensional sequence into a two-dimensional format. In this structure, binary values are mapped into a size of matrix, where the horizontal axis denotes as wavelengths, and the vertical axis corresponds to time slots (Matem et al. 2019).

Each binary '1' indicates an active transmission pulse, while a '0' signifies no data being sent. The outcome is a matrix where:

- *Rows* represent distinct wavelength channels (λ_1, λ_2, ..., λ_m), and
- *Columns* represent time intervals (t_1, t_2, ..., t_n).

This spatial-temporal configuration enhances the flexibility of user code allocation and significantly improves system performance in dense user environments. A typical 2-D Modified-FCC code is characterized by:

- M: number of wavelength (rows),
- N: number of time slots (columns),
- W: code weight (total number of ones),
- λ_a: auto-correlation,
- λ_c: cross-correlation.

Once the codewords are constructed using this matrix layout, the next step involves analyzing their cross-correlation behaviour to evaluate interference mitigation performance in the OCDMA link. Table 1 illustrates the 2-D Modified-FCC code constructions mapping based on a systematic approach that organizes the wavelength and time coefficients effectively.

TABLE 1. 2-D Modified-FCC Code Mapping between Wavelength and Time

		Wavelength (λ)																										
		X_0									X_1									X_2								
		0	0	0	0	1	1	0	1	1	0	1	1	0	0	0	1	1	0	1	1	0	1	1	0	0	0	0
	1	0	0	0	0	1	1	0	1	1	0	1	1	0	0	0	1	1	0	1	1	0	1	1	0	0	0	0
	0	0	0	0	0	0	0	0	0	0	0	0	0	0	0	0	0	0	0	0	0	0	0	0	0	0	0	0
	0	0	0	0	0	0	0	0	0	0	0	0	0	0	0	0	0	0	0	0	0	0	0	0	0	0	0	0
Y_0^T	1	0	0	0	0	1	1	0	1	1	0	1	1	0	0	0	1	1	0	1	1	0	1	1	0	0	0	0
	1	0	0	0	0	1	1	0	1	1	0	1	1	0	0	0	1	1	0	1	1	0	1	1	0	0	0	0
	0	0	0	0	0	0	0	0	0	0	0	0	0	0	0	0	0	0	0	0	0	0	0	0	0	0	0	0
	0	0	0	0	0	0	0	0	0	0	0	0	0	0	0	0	0	0	0	0	0	0	0	0	0	0	0	0
Time (t)	0	0	0	0	0	0	0	0	0	0	0	0	0	0	0	0	0	0	0	0	0	0	0	0	0	0	0	0
	1	0	0	0	0	1	1	0	1	1	0	1	1	0	0	0	1	1	0	1	1	0	1	1	0	0	0	0
	0	0	0	0	0	0	0	0	0	0	0	0	0	0	0	0	0	0	0	0	0	0	0	0	0	0	0	0
Y_1^T	0	0	0	0	0	0	0	0	0	0	0	0	0	0	0	0	0	0	0	0	0	0	0	0	0	0	0	0
	1	0	0	0	0	1	1	0	1	1	0	1	1	0	0	0	1	1	0	1	1	0	1	1	0	0	0	0
	1	0	0	0	0	1	1	0	1	1	0	1	1	0	0	0	1	1	0	1	1	0	1	1	0	0	0	0
	0	0	0	0	0	0	0	0	0	0	0	0	0	0	0	0	0	0	0	0	0	0	0	0	0	0	0	0
	0	0	0	0	0	0	0	0	0	0	0	0	0	0	0	0	0	0	0	0	0	0	0	0	0	0	0	0
	0	0	0	0	0	0	0	0	0	0	0	0	0	0	0	0	0	0	0	0	0	0	0	0	0	0	0	0
	1	0	0	0	0	1	1	0	1	1	0	1	1	0	0	0	1	1	0	1	1	0	1	1	0	0	0	0
Y_2^T	0	0	0	0	0	0	0	0	0	0	0	0	0	0	0	0	0	0	0	0	0	0	0	0	0	0	0	0
	0	0	0	0	0	0	0	0	0	0	0	0	0	0	0	0	0	0	0	0	0	0	0	0	0	0	0	0
	1	0	0	0	0	1	1	0	1	1	0	1	1	0	0	0	1	1	0	1	1	0	1	1	0	0	0	0
	1	0	0	0	0	1	1	0	1	1	0	1	1	0	0	0	1	1	0	1	1	0	1	1	0	0	0	0

2-D MODIFIED-FCC CODE PROPERTIES

To examine the interference-handling capability of the 2-D Modified-FCC codes, four characteristic correlation matrices, denoted as A(d), are generated. These matrices capture the interaction between different code sequences under varying shifts, with d ∈ {0, 1, 2, 3} representing the types of correlation shifts considered the matrices are calculated using the binary row vectors *X* and *Y*, which define the wavelength-time code entries. The general from are

$$A^{(0)} = XY^T \tag{7}$$

$A^{(1)}$, $A^{(2)}$, $A^{(3)}$ apply shifted and complemented operations to model different cross-correlation conditions.

The interference between any two users can then be quantified by the correlation function $R^{(d)}(g,h)$, where *g* and *h* represent shift indices in the wavelength and time domains respectively:

$$R^{(d)}(g,h) = \sum_{i=0}^{M-1} \sum_{j=0}^{N-1} a_{ij}^{(d)} a_{(i+g)(j+h)} \tag{8}$$

These functions are critical for assessing the system's resilience against MAI. The derived correlation values are tabulated and compared under various shift scenarios to ensure that the code performs optimally with minimal interference and noise, even as user count increases.

TABLE 2. Cross-Correlation Properties of the 2-D Modified-FCC

Input Condition (g, h)	(R_base)	(R_function1)	(R_function2)	(R_function3)
Case 1: g=0, h=0	k_1- k_2	0	0	0
Case 2: g=0, h=1	k_1	0	$k_1(k_2-1)$	0
Case 3: g=1, h=0	k_2	$k_2(k_1-1)$	0	0
Case 4: g=1, h=1	1	k_1-1	k_2-1	$(k_1-1)(k_2-1)$

As shown in Table 2, these properties play a critical role in mitigating MAI and suppressing the effects of PIIN. The derivation of the new correlation architecture coefficients is presented as follows (Cherifi et al. 2021).

$$R^{(0)}(g,h)-R^{(1)}(g,h)-\frac{R^{(2)}(g,h)}{(k_1-1)}+\frac{R^{(3)}(g,h)}{(k_1-1)} = \begin{cases} k_1k_2, & for \quad g=0 \; and \; h=0 \\ 0, & otherwise \end{cases} \tag{9}$$

This newly formulated 2-D Modified-FCC cross-correlation function is employed for MAI cancellation and PIIN suppression within overall OCDMA scheme. It is important to note that not all one-dimensional codes can be extended into wavelength–time code sequences, as many fail to satisfy the required cross-correlation properties for two-dimensional construction.

MAI ARCHITECTURE USING 2-D MODIFIED-FCC DESIGN

The proposed MAI suppression scheme is structured around the use of a 2-D Modified-FCC coding mechanism in an OCDMA system. Figure 1 illustrates the complete transceiver framework, which integrates several critical optical components at both the transmitting and receiving ends. Each transceiver unit consists of a continuous wave light source, an external modulator (such as a Mach-Zehnder modulator), multiplexing and demultiplexing modules, optical branching circuits, wavelength-selective elements like Fiber Bragg Gratings (FBGs), and photodetectors. Additionally, a subtraction mechanism is incorporated to enhance the decoding process by eliminating overlapping code signals from unintended users. Data encoding is performed using a binary modulation format, where an optical pulse is emitted only when the input bit is logical '1'. This is typically implemented using 2-level Amplitude Shift Keying (2-ASK), where '0' results in no optical output. This selective transmission ensures minimal interference within the shared medium.

At the receiving end, the decoder selectively filters the incoming signals based on the assigned wavelength-time code. Only when the temporal and spectral conditions match does the desired pulse pass through the decoding filters and get detected by the photodetector.

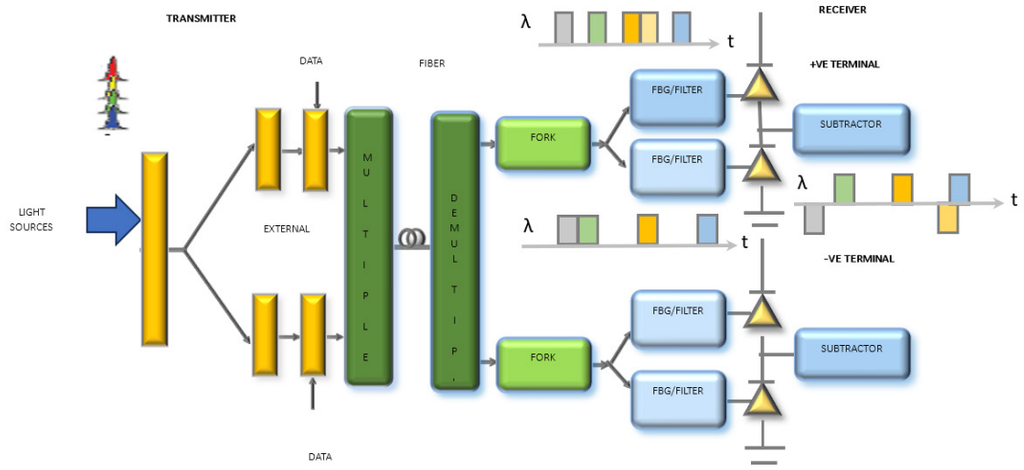

FIGURE 1. The 2-D Modified-FCC Interference Mitigation Diagram

To further suppress MAI, a logical AND-based subtraction is performed. In this method, the system compares two timeslot sequences and subtracts overlapping patterns using Boolean operations. For instance, if t_1 = [1100] and t_2 = [0110], the logical AND results in [0100], and the outcome of the subtraction process cancels out residual interference effectively.

By combining precise spectral-temporal filtering with Boolean suppression techniques, the 2-D Modified-FCC architecture significantly enhances resistance against noises effects. This leads to improved signal integrity, higher detection accuracy, and better system performance in high-density user environments.

TABLE 3. The 2-D Modified-FCC Interference Mitigation & Complementary Detection Techniques

	2-D Modified-FCC Interference Mitigation Technique				Complementary Detection Technique			
	λ_4	λ_3	λ_2	λ_1	λ_4	λ_3	λ_2	λ_1
t_1	1	1	0	0	0	0	1	1
t_2	0	1	1	0	0	1	1	0
	$\Theta t_1 . t_2 = 1$				$\Theta_{XY} = 1$			
	$t_1 \& t_2 = 0100$				X = 0010			
	$\Theta_{(t_1 \& t_2)} t_2 = 1$				$\Theta_{XY} = 1$			
Z	$Z_{MAI} = \Theta t_1 . t_2 - \Theta_{(t_1 \& t_2)} t_2 = 0$				$Z_{COMPLEMENTARY} = \Theta_{XY} - \Theta_{XY} = 0$			

RESULTS AND DISCUSSION

NUMERICAL EVALUATION

In this analysis, noises in the system are the main components that are usually considered when assessing the SNR (Ullah et al. 2024). The incoming optical signal, including thermal light, is detected by a photodiode, which produces a photocurrent and noise in the process. The following is a mathematical expression for this photocurrent noise as mentioned by (Mrabet, 2020)

$$\{i^2\} = 2eIB_r + I^2 B_r \tau_c + \frac{4K_b T_n B_r}{R_L} \quad (10)$$

From the Equation (10), I present as an average photocurrent which is generated by the light source known as photodiode. Its value varies depending on the specific configuration of the system that has been developed. There are four assumptions that have been taken into consideration for the proposed algorithm by (Mohammed et al. 2022). The optical source is assumed to be unpolarized, with its power uniformly distributed across the bandwidth range of $\left[\left\{v_o - \frac{\Delta V}{2}\right\}, \left\{v_o + \frac{\Delta V}{2}\right\}\right]$ where ν_0 represents the central frequency, and $\left(\frac{\Delta V}{2}\right)$ denotes half of the bandwidth in hertz. The power spectrum is divided into segments of equal width. Additionally, all users are assumed to transmit with equal power levels to the receiver, and the bit streams from users are perfectly synchronized. An important parameter in noise performance analysis, particularly in systems affected by PIIN(Bouarfa et al. 2020), is the coherence time, denoted as τ_c. Coherence time represents the temporal duration over which an optical field maintains a predictable phase relationship. In the context of incoherent light sources, when multiple optical fields with random phase fluctuations are combined and incident on a photodetector, these phase fluctuations lead to variations in the detected optical intensity manifesting as PIIN. The coherence time, τ_c is related to the optical source's spectral width and can be derived as,

$$\tau_c = \frac{\int_0^\infty [S^2(f) df]}{\left[\int_0^\infty S(f) df\right]^2} \quad (11)$$

The $S(f)$ of the received optical signal is linked to the incoherent time. When incoherent light is used, random phase changes occur in the light waves. When these waves mix at the photodetector, they create unwanted fluctuations in intensity, known as PIIN. To make the noise analysis easier, a Gaussian approximation is often used. This is because the noise from thermal sources follows a negative binomial distribution, but under normal system conditions, it behaves similarly to a Gaussian distribution. Another constant parameter is listed in Table 4.

1. PIIN Noise

$$\frac{B_r R^2 P_{sr}^2}{2M\Delta f k_2^2 (MN-1)^2} \tag{12}$$

2. Shot Noise

$$\begin{aligned}\{\langle I_{Shot}^2 \rangle\} &= 2eB_r(I_0 + I_1 + I_2 + I_3) \\ &= 2eB_r \frac{RP_{SR}}{Mk_2(MN-1)}[I_0 + I_1 + I_2 + I_3]\end{aligned} \tag{13}$$

3. Thermal Noise

$$\langle I_{thermal}^2 \rangle = \frac{4K_b T_n B_r}{R_L} \tag{14}$$

As for the performance evaluation, the SNR and BER of the algorithm can be written as follows:

$$= \frac{\left\{\frac{\Re P_{sr}}{MK_2}[K_1]\right\}^2}{\left\{\frac{B_r \Re^2 P_{sr}^2}{2M\Delta f k_2^2 (MN-1)^2}[[K_1K_2(MN-1)]^2 + 2(K_1K_2)(MN-1)K_2(W-1)(N-1) + [K_2(W-1)(N-1)]^2\right\}} + \left\{2eB_r \frac{\Re P_{sr}}{Mk_2(MN-1)}\left\{\left[K_1K_2(MN-1) + k_1\left(\frac{1+K_2}{2}\right)(W-1)(M-1) + 2K_2(W-1)(N-1) + 4(W-1)(M-1)(N-1)\right\}\right\} + \left\{\frac{4K_b T_n B_r}{R_L}\right\}} \tag{15}$$

$$BER = \frac{1}{2} erfc\left\{\sqrt{\frac{SNR}{8}}\right\} \tag{16}$$

TABLE 4. Design parameters for performance analysis

No.	Parameters	Value
1.	Efficiency of photodetector	η=0.75
2.	Spectral width	Δλ=30 nm
3.	C-Band wavelength	λ=1550 nm
4.	Bandwidth, *BW*	*B*=311 MHz
5.	STM bit rate levels	Refer to STM-x
6.	Load resistor	R_L=1030 Ω
7.	Light speed, *C*	*C*=3×10^8 m/s
8.	Noise temperature, *Tn*	T_n =300 K

Equations (15) and (16) are instrumental in conducting a numerical performance analysis of the 2-D Modified-FCC OCDMA systems. The parameters outlined in Table 4 are subsequently utilized to generate numerical results, thereby supporting the simulation-based performance evaluation presented herein.

Figure 2 illustrates the BER responds to variations in received optical power across several 2-D Modified-FCC configurations. In all tested scenarios, the spatial dimension was fixed at N = 6, while the spectral dimension M was varied. The trend shows a clear improvement in BER as the received power increases, attributed to the corresponding rise in noise ratio. Among the tested values, the configuration with M = 68 achieved optimal results, maintaining a BER of 10^{-9} at approximately -20 dBm. This highlights the codes strong potential for low-power, long-distance applications.

While other configurations such as M = 45 and M = 105 also demonstrated acceptable performance, their efficiency diminished at higher power levels likely due to insufficient redundancy shorter code or increased decoding complexity and noise accumulation longer code.

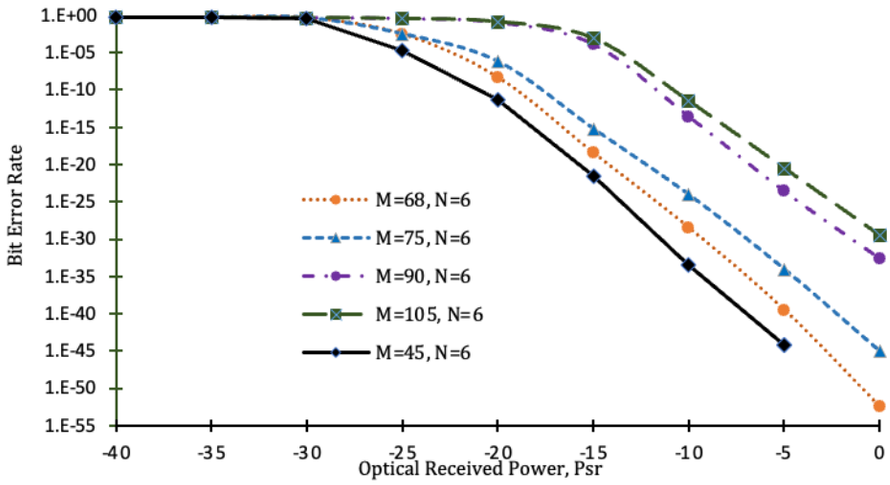

FIGURE 2. Impact of Optical Received Power (Psr) versus BER Performance at different lengths.

Figure 3 presents a comparative analysis between the proposed 2-D Modified-FCC and two existing OCDMA codes such as the 2-D MDW code and the 2-D PDC code. At bit rate of 1.1 Gbps, the 2-D Modified-FCC code significantly outperforms where it can supports up to 331 users with BER of 10^{-9}, whereas the MDW and PDC schemes can accommodate only 121 and 39 users respectively before their performance drops below acceptable thresholds. The enhanced user capacity of the proposed code is attributed to its improved cross-correlation characteristics and efficient interference suppression scheme. However, it is noted that increasing the bit rate or misaligning code sequences at the receiver can lead to higher cross-correlation effects, ultimately increasing interference and degrading the BER. Therefore, the 2-D Modified-FCC code offers a practical balance between user density and transmission quality, making it a strong candidate for scalable OCDMA systems where both high capacity and low error rates are critical.

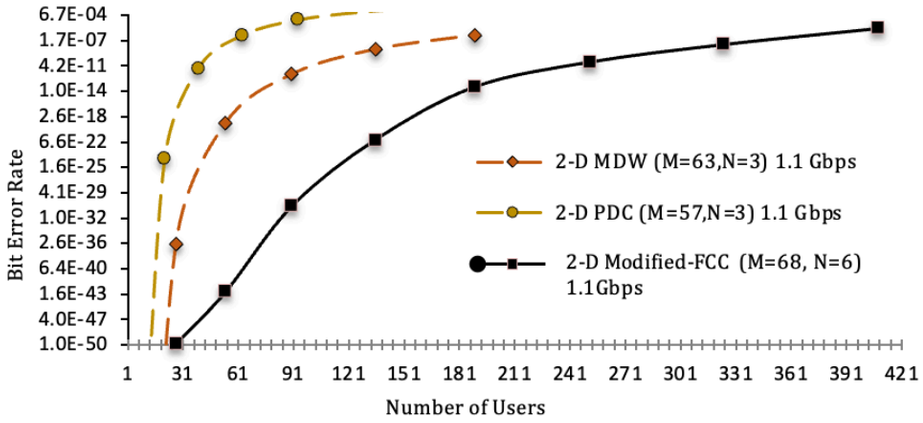

FIGURE 3. BER versus Number of Users with different spectral/spatial codes

SIMULATION ANALYSIS

To further evaluate the practicality of the 2-D Modified-FCC algorithm. The simulation model was developed using the OptiSystem platform as shown in Figure 4. The analysis focused on observing BER behavior across different fiber lengths: 10 km, 70 km, and 100 km, which represent short, medium, and long-haul optical transmission scenarios.

The transmitter block is composed of several core optical components arranged to replicate a realistic OCDMA signal generation environment. A random bit generator feeds into a pulse shaping unit. The optical carrier is provided by a continuous wave laser operating at a central wavelength of 1550 nm, modulated via a external modulator. A power combiner is then used to merge the encoded data before it is sent into the fibre channel. The optical link used single-mode fiber (SMF) segments of varying lengths, with parameters set to reflect typical fiber dispersion and attenuation values. No inline optical amplifiers or dispersion compensators are introduced, which allows a more direct evaluation of the codes intrinsic robustness. At the receiver end, the optical signal is separated using a wavelength-time demultiplexer tailored to the assigned code. A PIN photodetector captures the filtered signal, followed by a Bessel low-pass filter to smooth the waveform. The resulting electrical signal is analyzed using a BER analyzer and an eye diagram scope.

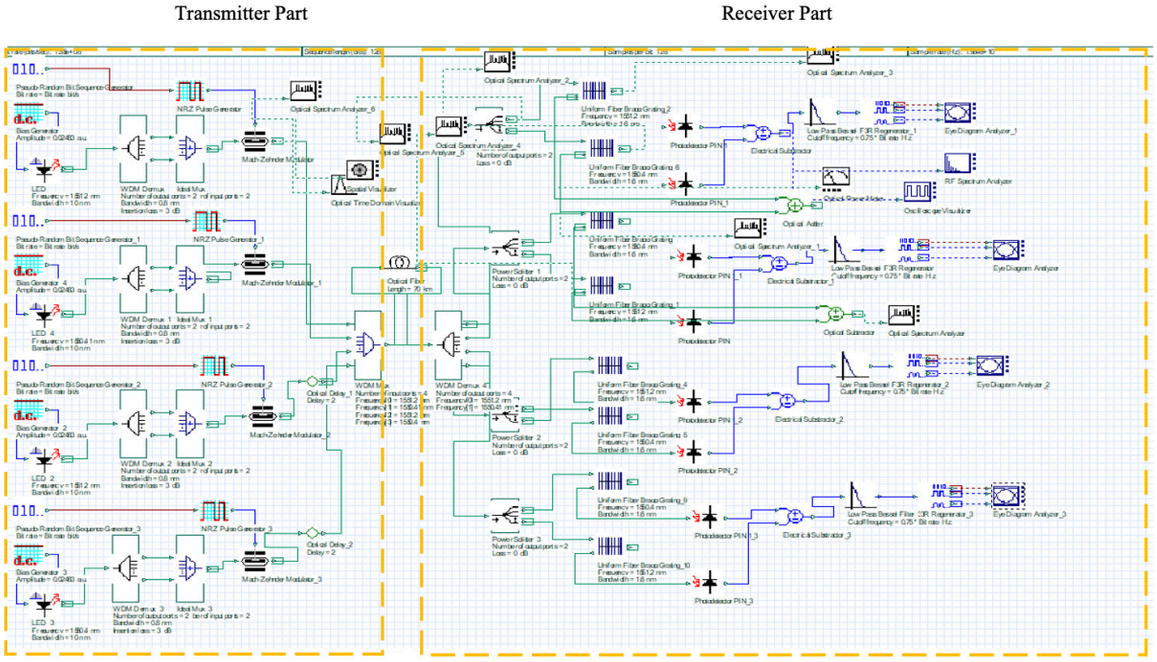

FIGURE 4. 2-D Modified-FCC Transceiver Design

Figure 5 (a)–(c) illustrate the eye diagrams and corresponding BER performance for distances of 10 km, 70 km, and 100 km, respectively. The measured BER values for four users operating at 1.1 Gbps are 1.272×10^{-25}, 1.166×10^{-21}, and 4.583×10^{-9}, respectively. As expected, an increase in transmission distance results in signal degradation due to cumulative effects such as chromatic dispersion and fiber attenuation, leading to a noticeable deterioration in both BER performance and eye pattern clarity. Nonetheless, by leveraging the 2-D Modified-FCC code arrangement, the 2-D Modified-FCC OCDMA system demonstrates a significantly enhanced BER performance at 100 km without the need for optical amplification or repeater elements. This underscores the effectiveness of the 2-D Modified-FCC coding arrangement in mitigating long-distance transmission impairments.

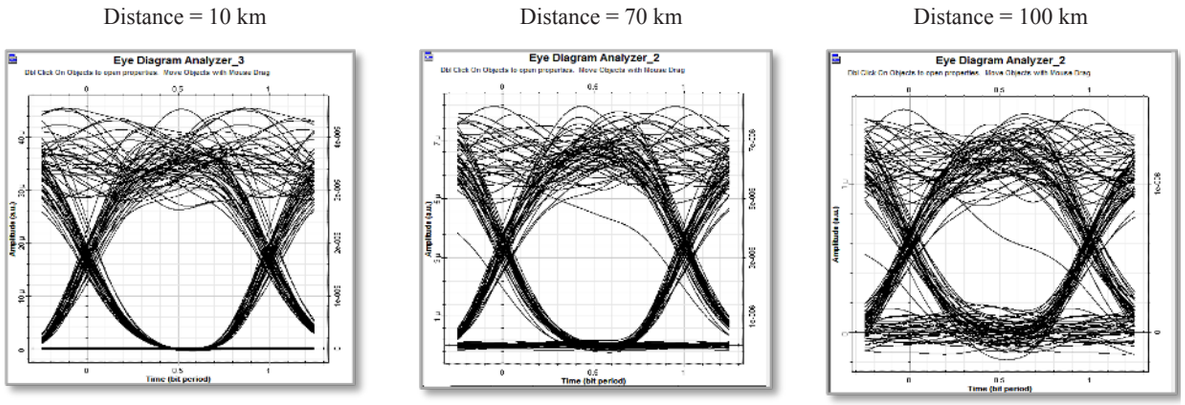

(a). Min BER = 1.272×10^{-25} (b). Min BER = 1.166×10^{-21} (c). Min BER = 4.583×10^{-9}

FIGURE 5. 2-D Modified-FCC Eye Diagrams

Figure 6 presents the comparison between fiber length and BER performance of the 2-D Modified FCC code at data rates of 1.1 Gbps and 2.5 Gbps. For a BER of 10^{-9}, the code achieves reliable transmission at 1.1 Gbps for distances up to 70 km. At 2.5 Gbps, the eye is narrower, but the system still provides reliable detection of ones and zeros, proving that the code works effectively even at higher speeds. From this observation, 2-D Modified FCC code performs strongly in both cases supporting long distances at 1.1 Gbps and ensuring reliable performance at higher bit rates of 2.5 Gbps. This highlights the codes flexibility and its ability to suppress PIIN and MAI effects in spectral/spatial OCDMA systems.

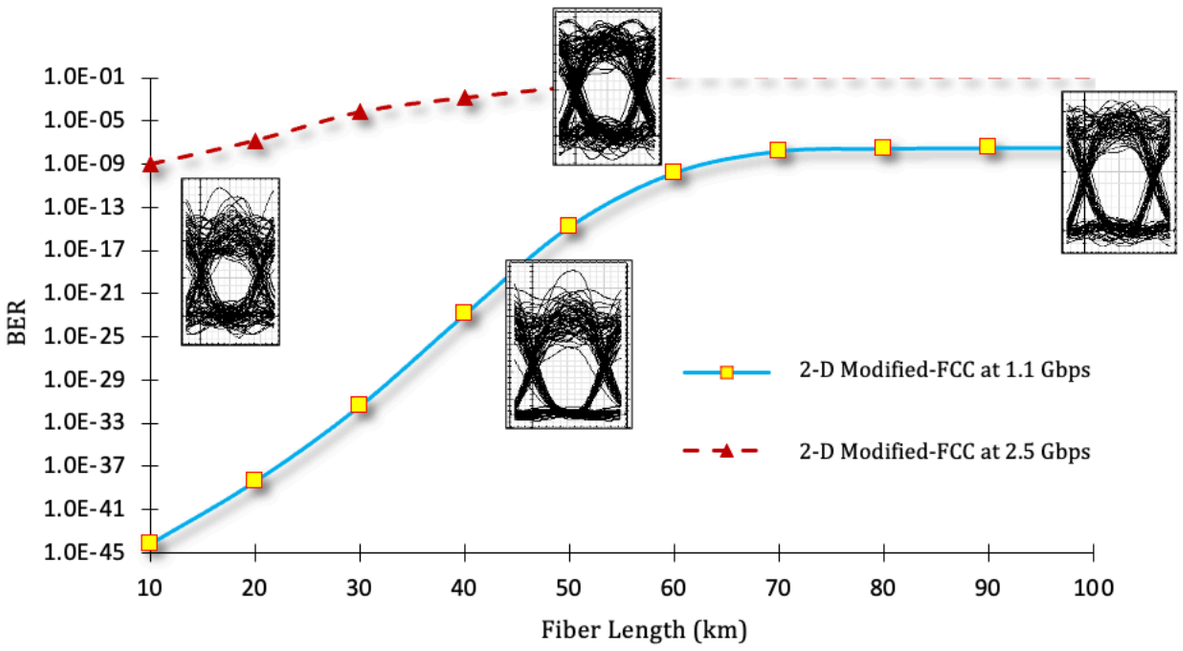

FIGURE 6. Bit rates performance on fiber length for 2-D Modified FCC code.

Figure 7 shows a comparison between the theoretical and simulation results of the 2-D Modified FCC code at different bit rates over a fixed fiber length of 70 km. At a BER of 10^{-9}, the theoretical result can support up to 1.1 Gbps, while the simulation achieves reliable performance up to 622 Mbps. The small difference between the two results happens because the theoretical model does not include effects like dispersion and attenuation, while the

simulation is simplified and mainly focused on Back-to-Back (B2B) transmission. Overall, the results show that both theory and simulation match well, proving that the 2-D Modified FCC code can perform reliably at different bit rates and that the simulation successfully supports the theoretical analysis.

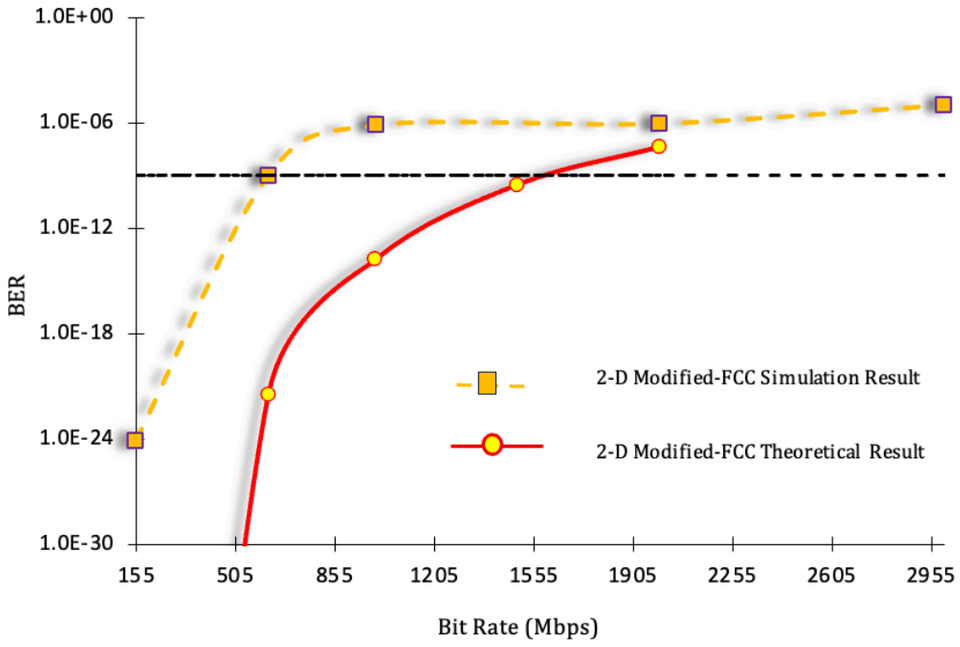

FIGURE 7. Comparison between theoretical and simulation results for 2-D Modified FCC code at various bit rates.

CONCLUSION

This paper has presented a comprehensive approach effectively mitigates critical limiting factors such as PIIN and MAI, leading to a substantial enhancement in overall system performance. A key indicator of this improvement is the remarkable increase in user capacity at BER = 10^{-9}. The system can accommodate an impressive 331 users, far surpassing the capacities of existing 2-D MDW (135 users) and 2-D PDC (39 users) codes. Beyond user capacity, the system demonstrates robust transmission capabilities. The 2-D Modified-FCC code, coupled with alleviation, achieves reliable bit rate of 1.1 Gbps at 70 km fiber link in a point-to-multipoint configuration, notably without the need for repeaters. This extended reach is further supported by a low optical receiver sensitivity of -20 dBm, indicating the receiver's efficiency in detecting weak optical signals over long distances. The effectiveness of the scheme in managing MAI is further substantiated by extremely low BER values for four users operating simultaneously at 1.1 Gbps, specifically 1.272×10^{-25}, 1.166×10^{-21}, and 4.583×10^{-9}, respectively. Additionally, the observed open eye diagram signifies excellent signal quality, underscoring minimal inter-symbol interference and effective noise suppression.

Finally, the 2-D Modified-FCC code algorithm represents a highly promising solution for the development of high-capacity, low-interference OCDMA systems. It demonstrated superiority in user support, extended repeater-less transmission distance at practical bit rates, and efficient optical receiver sensitivity collectively highlights its potential to satisfy the requirements of optical access systems of the future.

ACKNOWLEDGEMENT

The author would like to acknowledge the support from the Fundamental Research Grant Scheme (FRGS) under a grant number of FRGS/1/2022/TK07/UNIMAP/02/82 from the Ministry of Education Malaysia.

DECLARATION OF COMPETING INTEREST

None.

REFERENCES

Abuhelala, M., Korai, U. A., Sanches, A. L., Kwong, W. C. & Glesk, I. 2020. Investigation of 2D-WH/TS OCDMA code stability in systems with SOA-based device. *Applied Sciences* 10(21): 7943. https://doi.org/10.3390/app10217943

Alayedi, M., Cherifi, A., Hamida, A. F., Rahmani, M., Attalah, Y. & Bouazza, B. S. 2024. Design improvement to reduce noise effect in CDMA multiple access optical systems based on new (2-D) code using spectral/spatial half-matrix technique. *Journal of Optical Communications* 44(s1): s1265–s1276. https://doi.org/10.1515/joc-2020-0069

Bouarfa, A., Kandouci, M., Garadi, A. & Djellab, H. 2020. PIIN cancellation using a novel receiving architecture for spectral/spatial SAC-OCDMA system. *Journal of Optical Communications* 41(3): 295–304. https://doi.org/10.1515/joc-2017-0179

Boukricha, S., Ghoumid, K., Mekaoui, S., Ar-Reyouchi, E., Bourouina, H. & Yahiaoui, R. 2020. SAC-OCDMA system performance using narrowband Bragg filter encoders and decoders. *SN Applied Sciences*. https://doi.org/10.1007/s42452-020-2700-9

Cherifi, A., Bouazza, B. S., Alayedi, M., Aljunid, S. A. & Rashidi, C. B. M. 2021. Development and performance improvement of a new two-dimensional spectral/spatial code using the Pascal triangle rule for OCDMA system. *Journal of Optical Communications* 42(1): 149–158. https://doi.org/10.1515/joc-2018-0052

Das, N., Islam, Md. J. & Guho, A. 2022. Comparison of different codes on the performance of SAC-OCDMA over FSO link. 2022 International Conference on Recent Progresses in Science, Engineering and Technology (ICRPSET): 1–4. https://doi.org/10.1109/ICRPSET57982.2022.10188539

Din Keraf, N., Aljunid, S. A., Arief, A. R., Anuar, M. S., Rashidi, C. B. M., Ehkan, P. & Nurol, M. N. 2014. An optimal cardinality of wavelength/time incoherent OCDMA system using 2-D hybrid FCC-MDW code. 2014 2nd International Conference on Electronic Design (ICED): 356–361. https://doi.org/10.1109/ICED.2014.7015830

Islam, Md. R., Chandro, P., Sarkar, M., Ahmed, S., Bhuyan, Md. S. & Mukit Hassan, Md. 2022. Impact of inclination angle on the performance of UW spectral/spatial 2D-OCDMA system. 2022 13th International Conference on Computing Communication and Networking Technologies (ICCCNT): 1–6. https://doi.org/10.1109/ICCCNT54827.2022.9984514

Matem, R., Aljunid, S. A., Junita, M. N., Rashidi, C. B. M. & Ahmed, I. S. 2019. Photodetector effects on the performance of 2D spectral/spatial code in OCDMA system. *Optik* 178. https://doi.org/10.1016/j.ijleo.2018.10.068

Mizozoe, K., Matsumoto, T., Ohira, Y., Torii, H. & Ida, Y. 2023. Study on robustness to optical diffusion on undersea optical CDMA system using 2D optical ZCZ sequences. 2023 IEEE 12th Global Conference on Consumer Electronics (GCCE): 1090–1094. https://doi.org/10.1109/GCCE59613.2023.10315397

Mohammed, H. A., Abu Bakar, M. H., Anas, S. B. A., Mahdi, M. A. & Yaacob, M. H. 2022. Optical fiber sensor network integrating SAC-OCDMA and cladding modified optical fiber sensors coated with nanomaterial. *Optical Fiber Technology* 70: 102875. https://doi.org/10.1016/j.yofte.2022.102875

Morsy, M. A. 2022. Performance analysis of multi-rate coherent BPSK-OCDMA network for multimedia applications. 2022 8th International Engineering Conference on Sustainable Technology and Development (IEC): 179–184. https://doi.org/10.1109/IEC54822.2022.9807589

Mrabet, H. 2020. A performance analysis of a hybrid OCDMA-PON configuration based on IM/DD fast-OFDM technique for access network. *Applied Sciences*. https://doi.org/10.3390/app10217690

Rashidi, C. B. M., Aljunid, S. A., Ghani, F., Anuar, M. S. & Fadhil, H. A. 2012. Code length optimization using flexible cross correlation (FCC) code in OCDMA networks. 2012 IEEE 3rd International Conference on Photonics: 355–359. https://doi.org/10.1109/ICP.2012.6379828

Redouane, B., Fatima, B., Mohammed, C., Mehdi, D. & Abdelhakim, B. 2022. A high performance hybrid two dimensional spectral/spatial NZCC/MD code for SAC-OCDMA systems with SDD detection. *International Journal of Computer Networks & Communications* 14(2): 61–75. https://doi.org/10.5121/ijcnc.2022.14204

Tseng, S.-M., Chang, C.-K., Liu, M.-Y. & Wang, Y.-C. 2021. Throughput analysis of 2-D OCDMA/pure ALOHA networks with access control and two user classes of variable length for multimedia traffic. *Optik* 241: 166928. https://doi.org/10.1016/j.ijleo.2021.166928

Ullah, R., Ullah, S., Imtiaz, W. A., Alatawi, A. A., Alzaid, Z. & Alwageed, H. S. 2024. Optimization and analysis of spectral/spatial optical code division multiple access passive optical network. *AEU – International Journal of Electronics and Communications* 175: 155084. https://doi.org/10.1016/j.aeue.2023.155084

Yousif Ahmed, H., Zeghid, M., Imtiaz, W. A., Sharma, T., Chehri, A. & Fortier, P. 2020. Two-dimensional permutation vectors (PV) code for optical code division multiple access systems. *Entropy* 22(5): 576. https://doi.org/10.3390/e22050576